Title

THE TRAPPING OF CHARGED PARTICLES IN AXIALLY SYMMETRICAL SYSTEMS OF ELECTRIC AND MAGNETIC FIELDS

Authors

Gow, J.D.
Ruby, L.
Smith, L.
et al.

Publication Date

1958-01-24

UNIVERSITY OF CALIFORNIA

Radiation Laboratory

BERKELEY, CALIFORNIA

DISCLAIMER

UNIVERSITY OF CALIFORNIA
Radiation Laboratory

Cover Sheet
Do not remove

INDEX NO. UCRL-8156
This document contains 34 pages
This is copy 9 of 15 series A
Date January 24 1958

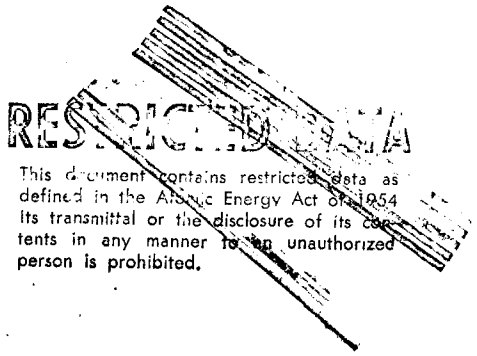

DECLASSIFIED

Issued to Information Division

Classification

Each person who receives this document must sign the cover sheet in the space below.

Route to	Noted by	Date	Route to	Noted by	Date
Patent Atty McRae		3-11-58			
	Thomas	3-11-58			
Re route to Patent !					
Art Rosen					
Mabel					

RL-220

UCRL-8156

UNIVERSITY OF CALIFORNIA
Radiation Laboratory
Berkeley, California

Contract No. W-7405-eng-48

THE TRAPPING OF CHARGED PARTICLES IN AXIALLY SYMMETRICAL SYSTEMS OF ELECTRIC AND MAGNETIC FIELDS

J. D. Gow, L. Ruby, L. Smith, and J. M. Wilcox

January 24, 1958

Printed for the U. S. Atomic Energy Commission

THE TRAPPING OF CHARGED PARTICLES IN AXIALLY SYMMETRICAL SYSTEMS OF ELECTRIC AND MAGNETIC FIELDS

by

J. D. Gow, L. Ruby, L. Smith, and J. M. Wilcox

Radiation Laboratory
University of California
Berkeley, California

An electron-trapping geometry is described which was accidentally observed in the course of a PIG ion-source development program. Some possible applications to the Sherwood program are discussed. The anode sheath formed at the central rod of a magnetronlike geometry is measured and analyzed.

I. EXPERIMENTAL OBSERVATIONS OF ELECTRON-TRAPPING GEOMETRY

We should like to begin by describing some experimental observations made in February and March of 1957, which have stimulated interest in the use of combined electric and magnetic fields for Sherwood purposes. In the course of a development program on PIG ion sources, it was discovered that the geometry shown in Fig. 1 could serve as an ion source capable of producing a pulsed beam of 1 ampere of protons. In order to produce an ampere of ion current, a current of the order of tens of amperes of ionizing electrons would be required. Since no such large currents were observed to flow from the cathode to the anode, we were forced to conclude that some trapping mechanism must be operating.

Consider a region of space containing an axially symmetric magnetic field having an axial gradient of the "z" component. Such a field combination is shown schematically in Fig. 1. Let us assume the electric field in such a direction as to accelerate a charged particle of given sign in the positive z direction, and $(d|B_z|/dz) > 0$ in the region between the electrodes. A charged particle, starting at a suitable

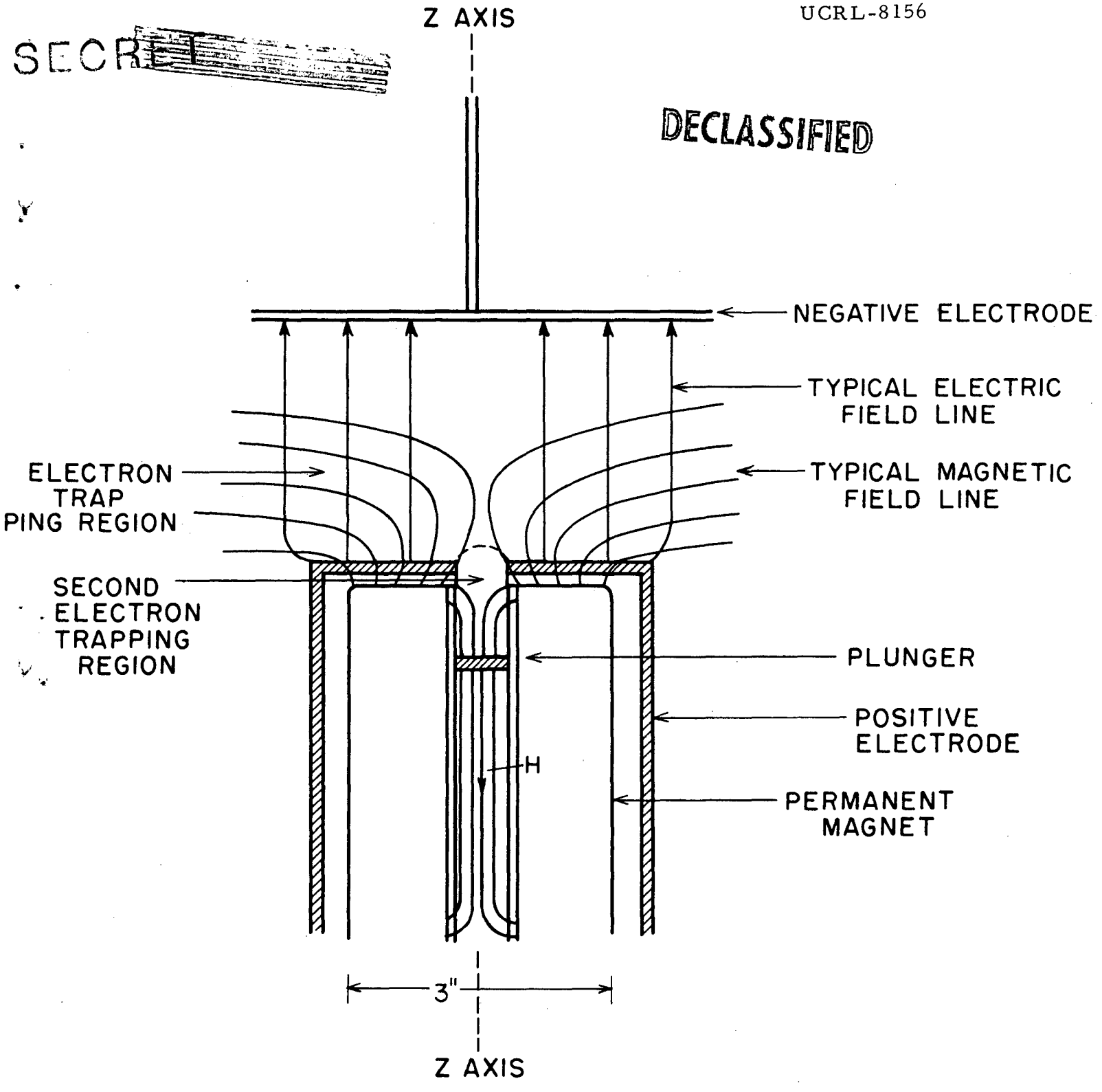

ARRANGEMENT OF ELECTRIC & MAGNETIC FIELDS

Fig. 1

value of r and accelerated into the region of increasing magnetic field, will cross the radial component of the magnetic field and, therefore, acquire a tangential component of velocity. This tangential motion is motion at right angles to the z component of the magnetic field, and results in a force tending to bend the particle trajectory around the z axis.

For physically realizable axially symmetric fields, B_r is zero on axis, increases to a maximum value for some value of the radius, and then again decreases. Thus, particles which start too near the axis will not be trapped. If the diverging magnetic field is that produced by a pole of a permanent magnet or by a current loop, B_z will reverse sign for sufficiently large radius. The radial force changes sign when B_z is reversed in sign with respect to B_r. Therefore, there will be a limiting outer radius beyond which trapping is impossible for any value of E. For suitable field configuration, electrons starting their motion in a range of radial positions between these limiting values can be trapped for a time that is very long compared with the period of oscillation.

If an electron is contained in the trapping region, it will eventually make an ionizing collision with a molecule of the gas. The time required for such a collision to occur in H_2 is essentially independent of the electron energy, since the ionization cross section for hydrogen varies inversely as the electron velocity over a wide range of velocity. As a result, the product of the ionization cross section σ_i and the electron velocity v is equal to 6×10^{-8} cm^3/sec for electrons with energy from 100 volts to 2000 volts.

At an operating pressure of 10 microns, the density of gas molecules is 3.5×10^{14} molecules/cc. The mean time between ionization events for moderately fast electrons in a 10-micron pressure of H_2 is given by

$$t_i = \frac{1}{N_{H_2} \sigma_i v} \cong 5 \times 10^{-8} \text{ sec.}$$

Thus, in a time of $\sim 5 \times 10^{-8}$ second, we would expect an ionization event to occur. The energy loss to the initial electron will, on the average, be very small compared with its kinetic energy, therefore its motion will not be appreciably disturbed. The electron liberated in the ionizing event is, by definition, liberated in the trapping region. It will take up a motion similar to that of the first electron.

The positive ion formed will be only slightly affected by the magnetic field, owing to its large mass. The ion will move to the negative electrode under the influence of the electric field, being deflected outward radially to a slight extent as it leaves the region of strong magnetic field.

Such a discharge will increase exponentially in intensity until limiting mechanisms appear, provided the trapping time for the electrons is long compared with the mean time between ionization events.

Under the latter assumption, the number of new electrons appearing per unit time in the trapping region will be proportional to the number present at any instant, divided by the mean time between electron-production events per electron, or

$$\frac{d N_e}{d t} = \frac{N_e}{N_H \sigma_i V},$$

or

$$N_e(t) = N_0 \, e^{\frac{t}{N_H \sigma_i V}}.$$

A diagram of the first apparatus arranged to explore the trapping effect is shown in Fig. 2, and Fig. 3 is a photograph of the device.

A set of nine Indox permanent-magnet rings was placed in a nonmagnetic stainless steel case, which was attached to a brass flange. This flange served as an end plate for a piece of 4-inch i.d. pyrex industrial glass pipe. A similar flange on the opposite end of the glass pipe served to support a disk electrode which could be moved in the axial direction.

Pumping and gas-inlet pipes passed through the magnet support flange. A tubulation mounting an ionization-gauge tube also passed through the same flange. Pumping was accomplished by means of a three-stage mercury diffusion pumping system with two stages of liquid nitrogen trapping interposed between the pump and the tube.

The pressure in the tube could be adjusted to any convenient value above the base pressure of the system, which was about 10^{-5} mm Hg.

The magnet case and flange normally were grounded through a resistor of 1 ohm, permitting observation of the tube current in terms of the voltage developed across the grounding resistor.

The flange supporting the disk electrode served as a high-voltage terminal. To this terminal negative potential was applied by means of a pulse transformer as the source of voltage. The peak voltage was continuously adjustable from zero up to a maximum of 250 kv. By variation of the primary drive network, the transformer could deliver pulses of various shapes and lengths. Typically, the pulse rise time was chosen to be about 3 microseconds, and the duration (full width at half maximum) about 6 μsec.

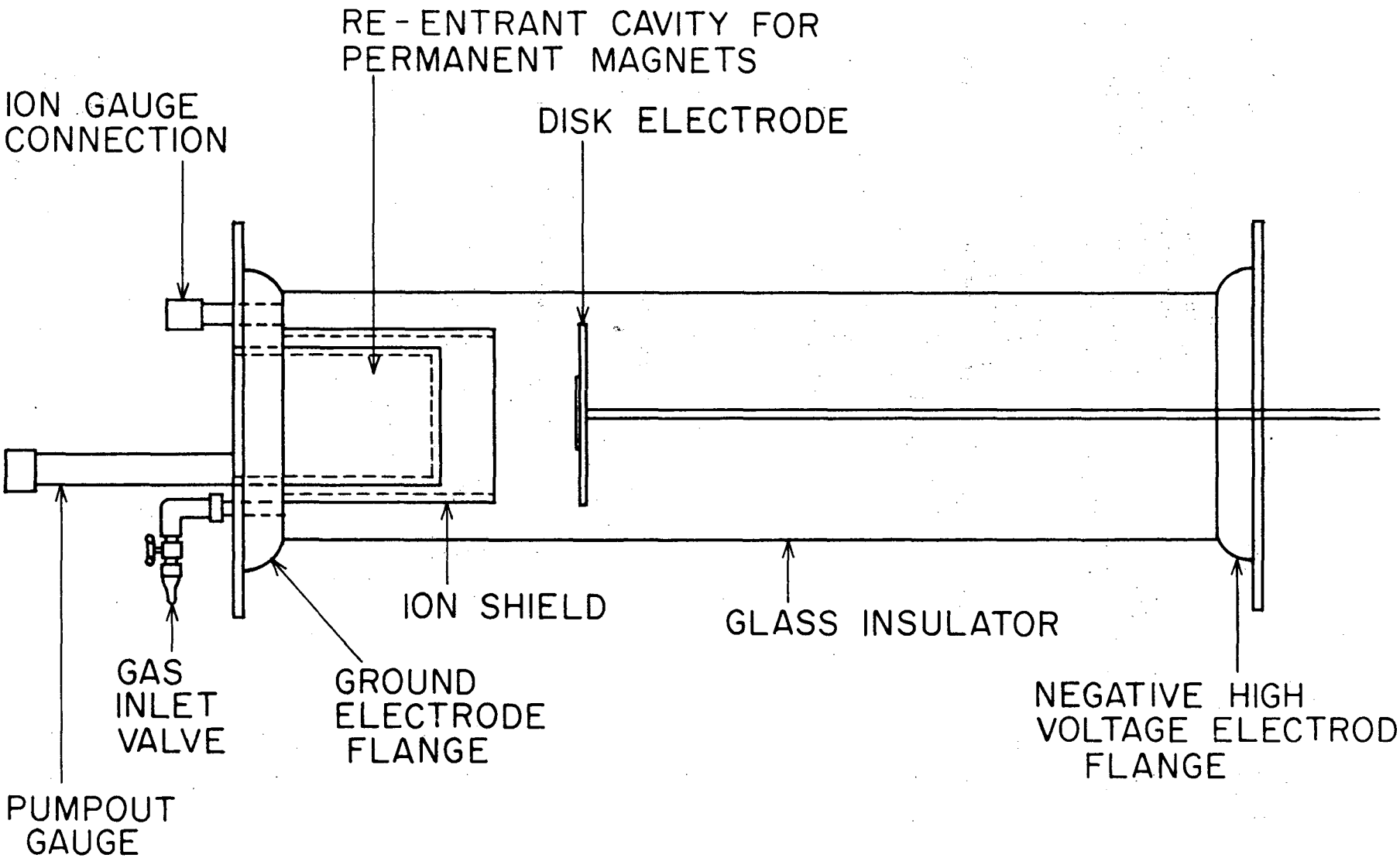
RE-ENTRANT CAVITY FOR
PERMANENT MAGNETS
ION GAUGE
CONNECTION
DISK ELECTRODE
ION SHIELD
GLASS INSULATOR
GAS
INLET
VALVE
GROUND
ELECTRODE
FLANGE
NEGATIVE HIGH
VOLTAGE ELECTRODE
FLANGE
PUMPOUT
GAUGE
UCRL-8156

Fig. 2

Fig. 3

A considerable range of interesting phenomena resulted when the device described above was placed in operation. It was found that upon application of negative potential to the disk, currents of several amperes flowed through the tube. The current proved to be a smooth function of both the operating pressure and the applied high voltage. It was demonstrated that an appreciable fraction (~ 10 to 20%) of the total current to the disk consisted of ions that had been accelerated through a potential drop approximately equal to the applied potential. A large flux of soft (~ 10-kv) x-ray emission was observed to come from the device.

The electrical characteristics of the device were found to be substantially unchanged when a solid cylindrical magnet was substituted for the hollow cylindrical magnet used in the first experiment. Although certain features of the discharge appeared quite different according to whether the central hole was covered at the pole surface or left open, it was demonstrated that the major effects observed were related to the combination of electric and magnetic fields in the space between the magnet case and the negative electrode.

The current density to the disk electrode was measured as a function of radius, and a substantially uniform current of positive ions was found to fall on the entire electrode surface.

The above phenomena were observed for hydrogen pressures in the range from 6 to 20 x 10^{-3} mm Hg in the device, where the mean free path for ionization is large compared with the tube dimensions.

When the magnet case in Figs. 2 and 3 was examined subsequent to the operation of the device, a heavily bombarded (damaged) spot was found at its center. The spot was about 3 mm in diameter. This observation led to the conclusion that most of the electrons leaving the discharge were closely confined about the s axis of the magnetic field as they escaped.

This loss could easily be eliminated when hollow magnets are used by merely leaving the central hole open and providing another negative electrode to face the opposite end of the magnet.

Such a device was constructed, and is shown schematically in Fig. 4. A photograph of the tube is shown in Fig. 5. The electron densities appeared (from measurement of the soft bremsstrahlung) to be considerably higher when this "double-ended" device was operated.

II. SHERWOOD APPLICATIONS: EXPERIMENTAL

Having arrived experimentally at an electron-trapping geometry, we wished to investigate its Sherwood possibilities. For the trapping of ions, larger magnetic fields and system dimensions would be needed. A machine using the largest components readily available was assembled.

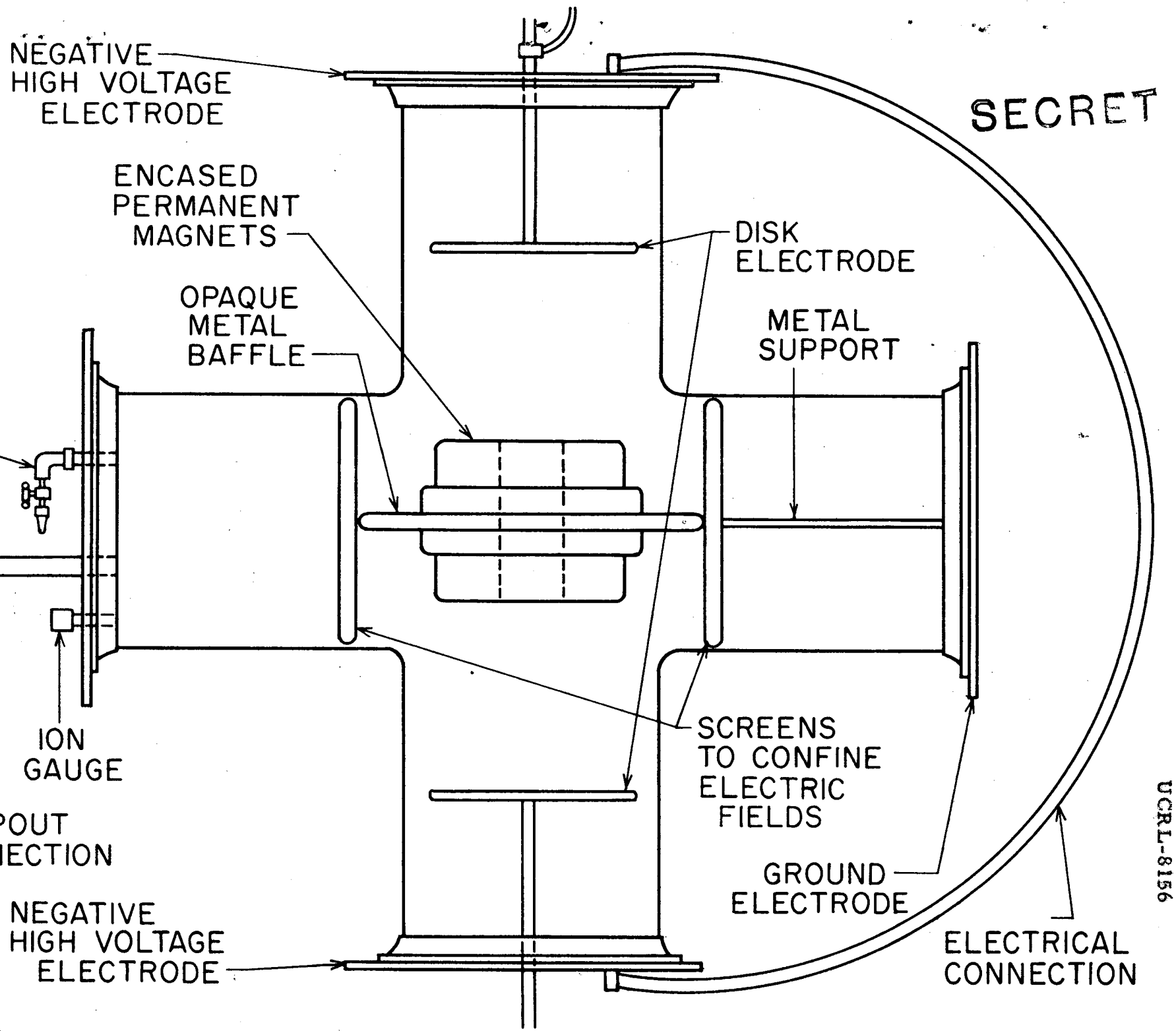

UCRL-8156

Fig. 4

50,608-I

Fig. 5

This machine, which became known as the Plus-One machine, is shown in Fig. 6. Pertinent specifications are as follows:

Magnet

Directly water-cooled; 14 sections, 27 turns per section. Iron flux-return bars on the outside coil surface.

Coil internal radius = 9 cm.

Coil external radius = 18 cm.

Width of each section = 1.2 cm and insulation.

Maximum available field at center of symmetry ≅ 3000 gauss (at 100 amperes).

Discharge Tube

Brass central pipe (throat), with brass flanges to hold pyrex bell jars.

Throat radius at center of symmetry = 7.5 cm.

Throat radius at flanges = 6.25 cm.

Bell jar radius = 38 cm.

Disk electrode radius = 26.7 cm.

Disk electrode separation: variable.

Vacuum System

Mercury diffusion pump with liquid nitrogen and refrigerated-baffle traps. Base pressure in tube on untrapped gauge ~ 10^{-6} mm Hg.

High-Voltage Supply

Pulse Transformer.

Voltage range = 0 to 150 kv.

Current available ~ 20 amperes maximum at 150 kv.

Pulse length = 100 microseconds.

Pulse rise time = 10 microseconds.

The drawing in Fig. 6 shows the Plus-One device with an axial conductor passing through the throat of the discharge tube. This

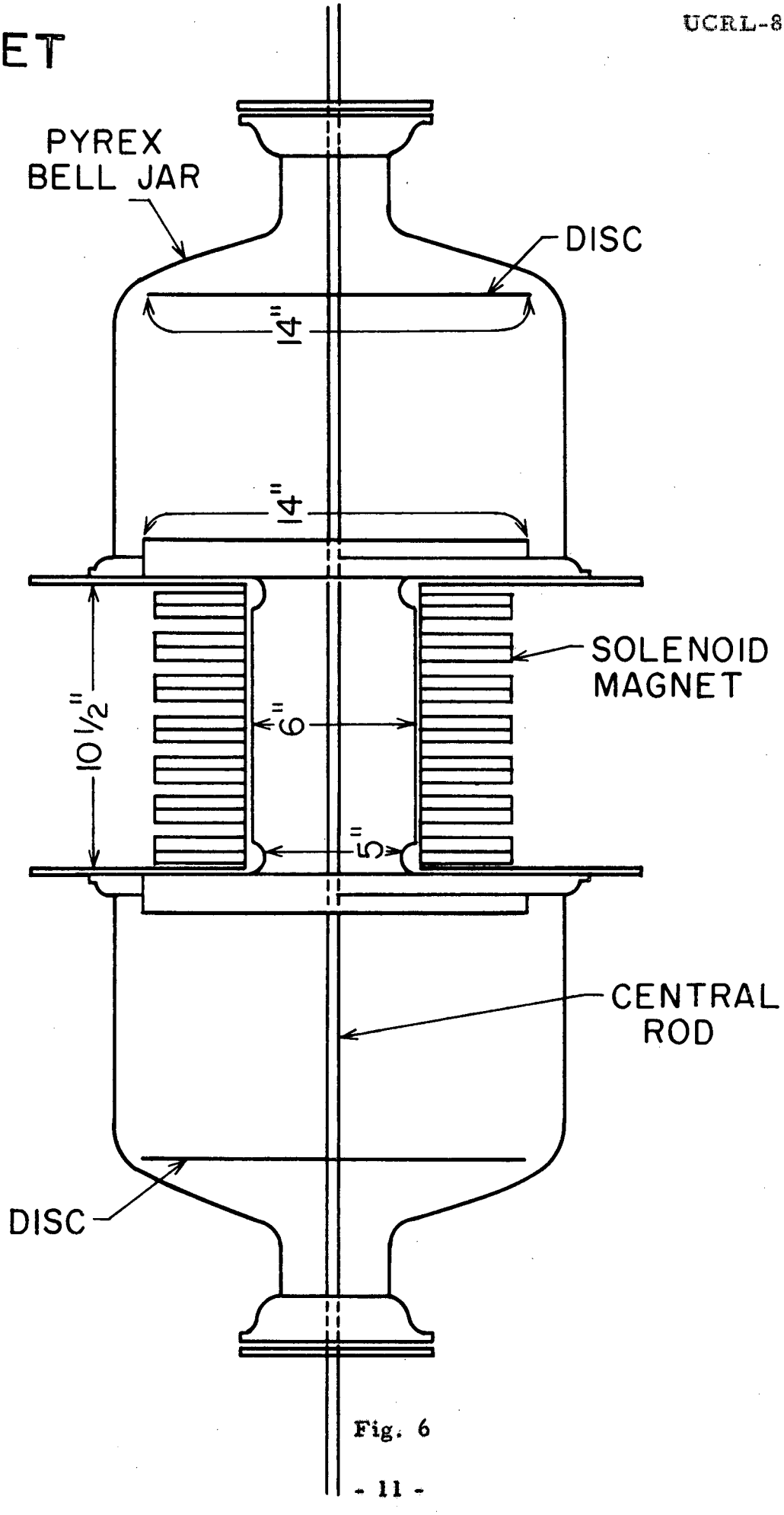
PYREX
BELL JAR
DISC
14"
14"
SOLENOID
MAGNET
10 1/2"
6"
5"
CENTRAL
ROD
DISC

Fig. 6

modification was added later, and was not present during the early operation of the machine. The reason for introducing the central rod will become apparent in the description of the experimental phenomena.

Plus-One Experiments

The initial approach to the Plus-One machine phenomena was highly empirical. The machine was pumped to as good a vacuum as possible and high voltage was applied, with positive polarity, to the end electrodes; the brass magnet case was returned to ground through a shunt which permitted oscillographic observation of the current. With a pressure of 10^{-6} mm Hg, the only current observed was that due to the charging of the capacitance between the high-voltage electrodes and the case. (This capacitance was later measured and found to be ~30 μμf.)

When deuterium was admitted, the current was found to increase substantially. The discharge could be made to occur for applied voltages ranging from ~30 kv up to the limit available. After an initial bake-in period, operation was found to be very steady (free of breakdown). Characteristics such as current versus voltage, current versus magnetic field, etc. were very reproducible.

The discharge appearance was as follows. Only a faint bluish glow was seen in the space between the positive electrodes and the magnet case, and much of this was probably due to the fluorescence of the glass. The throat region, however, gave a salmon-pink glow which appeared to extend entirely through the throat volume and terminate rather sharply in a curved boundary, extending about an inch into the space between the magnet case and the positive disks, and extending radially somewhat farther than the limiting aperture of the throat.

In early experiments, it was found that the color of this central glow depended on the purity of the deuterium in the machine. When an air leak or outgassing occurred, the glow changed to a bluish-pink appearance. Such a change was also accompanied by a reduction in the neutron output of the machine.

Neutron-Output Measurements

Neutron counting was accomplished by providing a large block of plastic scintillator close to the machine, the scintillator being viewed by four photomultiplier tubes in parallel. In order to avoid the possibility of electrical pickup or the counting of x-rays, the scaler that registered the photomultiplier impulses was gated off during the machine pulse and for about 50 microseconds thereafter. The scaler was then gated on for 150 microseconds. Counting depended on the storage of thermal neutrons in the block of scintillator, resulting from the thermalization of fast neutrons incident on the scintillator during the machine pulse. The actual counts observed were the capture of gamma rays resulting from

$$p + n \rightarrow d + \gamma + 2.2 \text{ Mev} .$$

The mean life of a thermal neutron in the plastic is ~ 130 microseconds for the size of block used (7 in. in diameter by 10 in. in length).

With this method, it was possible to detect easily a neutron yield of as little as 10^3 neutrons/pulse, provided ~ 1000 pulses were used to average out background fluctuations. A typical neutron-counter sensitivity was 1 count for each 2×10^4 neutrons emitted by the machine. Typical background was less than 0.01 count per gate.

Using the method of neutron counting described, we found that considerable neutron emission resulted from operation of the tube. The neutron output was a function of the magnetic field, the applied voltage, and the pressure of deuterium in the system.

The neutron yield as a function of operating pressure is shown in Fig. 7. It is seen that the yield is proportional to the square of the pressure up to an ion-gauge pressure of about 0.6 micron,* where a break occurs and the yield begins to rise much more rapidly with pressure. The tube current also rises very rapidly with pressure above 0.6 micron, and soon reaches the maximum value that the hv pulse transformer can supply. Figure 8 shows the neutron yield as a function of the high voltage applied to the tube. As the voltage is increased, the current drawn by the tube also increases. Therefore one divides the observed neutron yield by the tube current in order to present the variation of yield due only to changing voltage. The experimental points lie close to the solid line, which shows the nuclear cross section for singly ionized deuterium molecules bombarding a thin target.

The dependence of the neutron yield on the square of the pressure suggested that the reactions were taking place in the volume of the plasma, and not on the metal surfaces. In order to test this assumption, a proton counter capable of counting high-energy protons formed in the reaction

$$d + d \rightarrow t + p$$

was attached, on axis, to one end of the machine. An aperture in the positive disk electrode followed by a defining tube gave collimation such that only the 3-Mev protons produced in the throat volume could reach the counter. Protons resulting from d-d reactions anywhere on the surface of the magnet case were excluded from the counter by the collimating system. The protons were allowed to pass through a 1-mil Al diaphragm which served as a vacuum wall, and were then counted in a thin layer (~ .010 in.) of plastic scintillator viewed by a photomultiplier.

With this apparatus, counts coincident with the high-voltage pulse were obtained. The identification of the particles as protons was by

---

*Experimental measures of pressure are reported in ionization-gauge readings. To get the true pressure these readings must be multiplied by about $2\frac{1}{2}$.

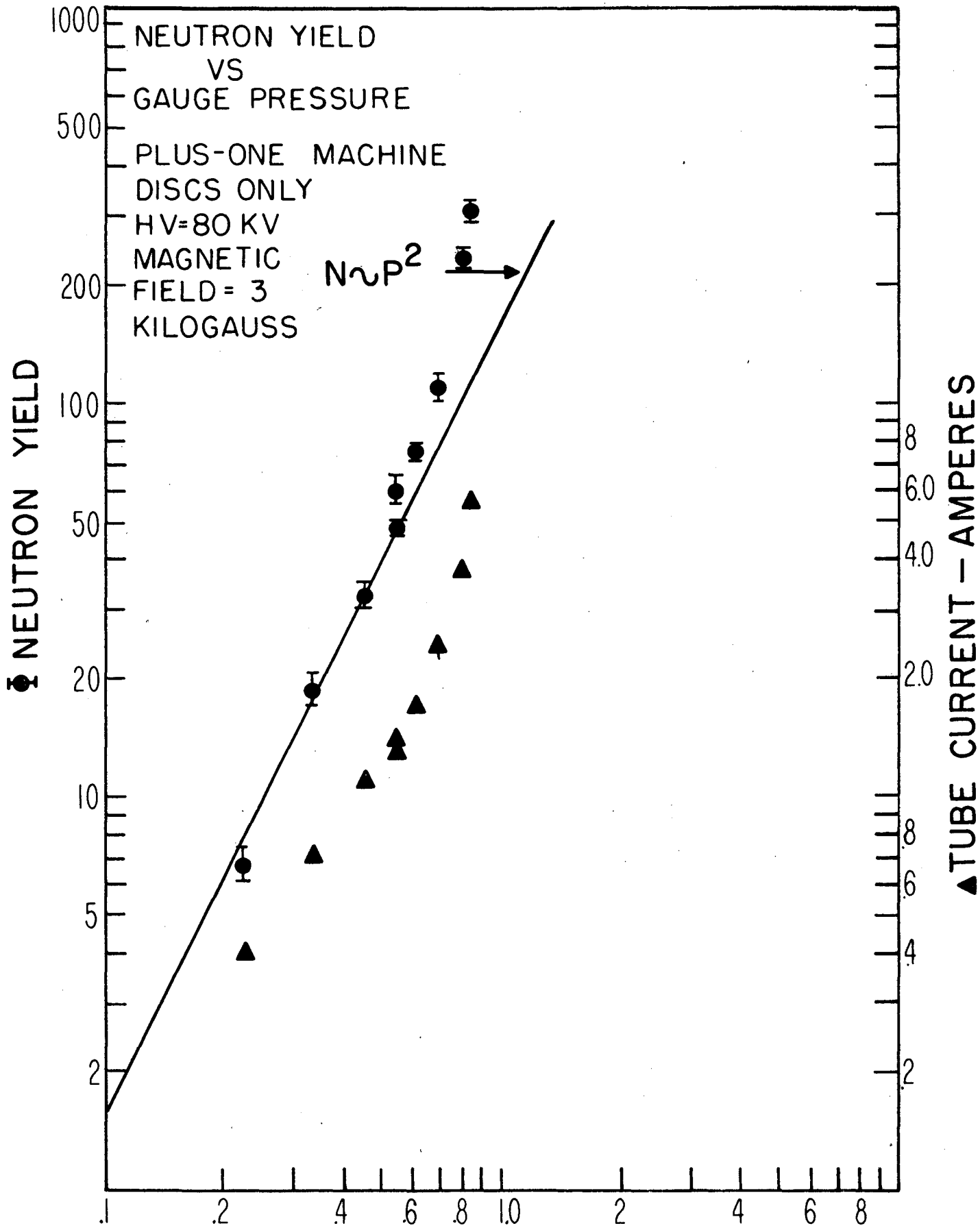
NEUTRON YIELD
VS
GAUGE PRESSURE
PLUS-ONE MACHINE
DISCS ONLY
HV=80 KV
MAGNETIC
FIELD = 3
KILOGAUSS
N∼P²
● NEUTRON YIELD
▲ TUBE CURRENT – AMPERES
1000
500
200
100
50
20
10
5
2
8
6.0
4.0
2.0
.8
.6
.4
.2
.1
.2
.4
.6
.8
1.0
2
4
6
8
PRESSURE – MICRONS
(ION GAUGE)

Fig. 7

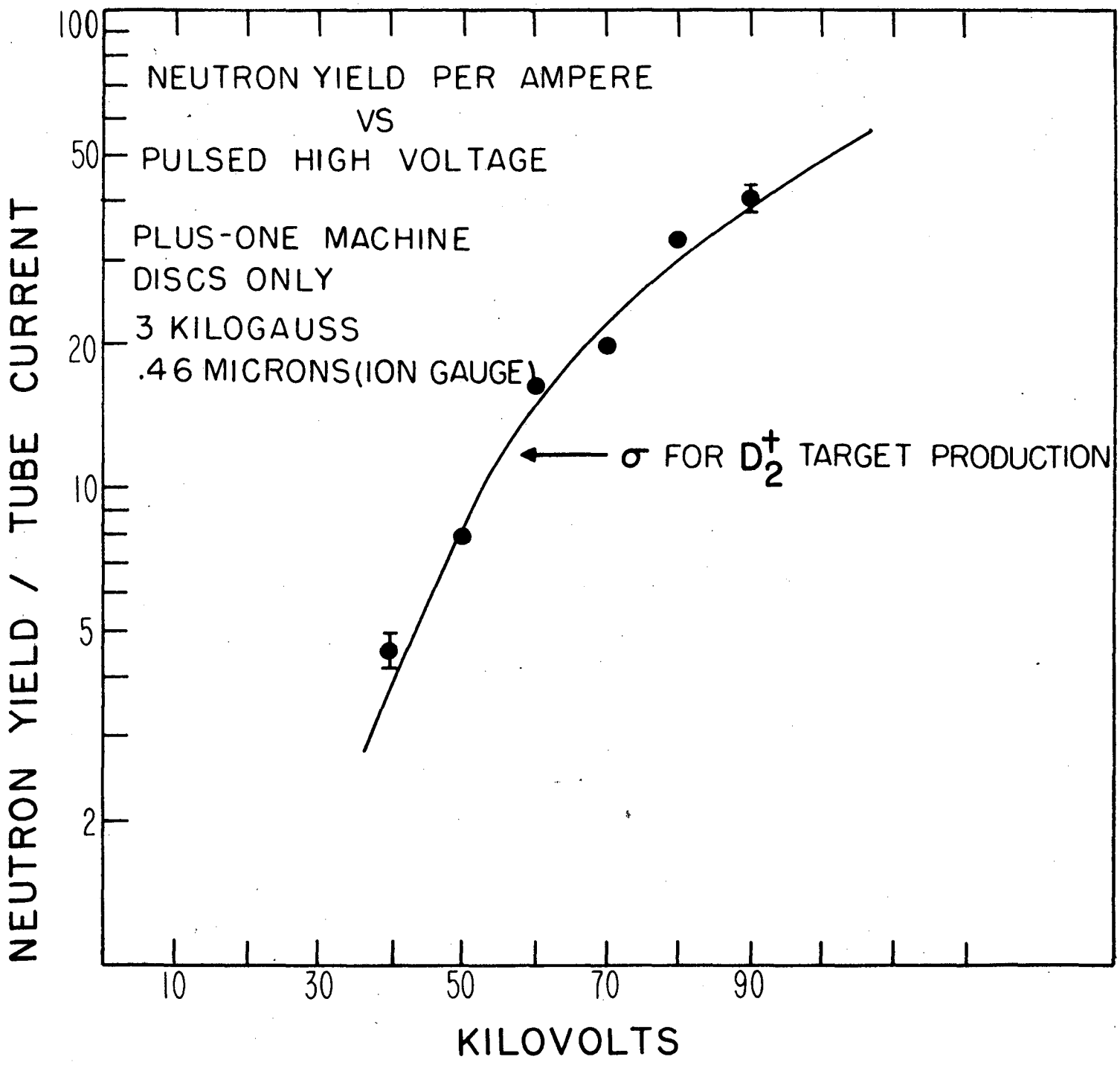
NEUTRON YIELD PER AMPERE
VS
PULSED HIGH VOLTAGE
PLUS-ONE MACHINE
DISCS ONLY
3 KILOGAUSS
.46 MICRONS(ION GAUGE)
σ FOR D_2^+ TARGET PRODUCTION
NEUTRON YIELD / TUBE CURRENT
100
50
20
10
5
2
10
30
50
70
90
KILOVOLTS

Fig. 8

means of their range in Al. The counts associated with the protons could be eliminated by the addition of 0.003 in. of additional Al absorber between the exit foil and the counter.

The yield of protons per pulse agreed quantitatively with the measured neutron output within the accuracy to which the calibration of the neutron counter was known. The ratio of the proton-counter signal rate to the neutron-counter signal rate was independent of variation of machine pressure or of operating voltage.

From these measurements, it was deduced that the d-d reactions producing the observed neutrons took place primarily in the volume of the throat and not on the surfaces.

The Sherwood Group at Los Alamos suggested that there was an effectively conducting axial region in Plus-One surrounded by a radial sheath (see Section III). If this hypothesis is correct, the replacement of the central magnetic conduction effect by a solid metallic rod extending along the axis of the machine should not upset the system.

A 3/8-inch stainless steel rod was installed (as previously mentioned) as shown in Fig. 6. After the installation of this rod, comparable phenomena were encountered at an applied potential a few kilovolts lower than without the rod. There was no change in the visual appearance of the discharge, in the magnitudes of the current observed, or in the relative neutron output for a given applied voltage and magnetic field.

For Plus-One with central rod, the neutron yield varies as the pressure to the power 1.27, as shown in Fig. 9. The neutron yield versus magnetic field is shown in Fig. 10. The neutron yield as a function of high voltage is very close to the D_2^+ cross section curve, as was the case without the central rod.

Some data were taken with the central rod in place and the end discs removed. In this case the neutron yield, tube current, and x-ray production increased by an order of magnitude. The neutron yield versus high voltage followed the D_2^+ cross section curve, as shown in Fig. 11.

Two pickup electrodes (fins) were installed in Plus-One with discs only, as shown in Fig. 12, and the charge striking them was displayed on a dual-trace oscilloscope. The fins were shielded by a guard so that radially moving particles could not hit them. With the magnetic field in a direction such that positive ions would strike fin A, the negative signal on fin A was about 0.2 milliampere and the negative signal on fin B was about 0.3 ma. The total radial tube current was 20 ma. When the central rod was installed in Plus-One, the positive signal on fin A was about 4 ma and the positive signal on fin B was about 1 ma, while the radial tube current increased to 1 amp. When the direction of the magnetic field was reversed, the signals appearing on A and B were interchanged. These results could indicate the presence of ions in magnetron-like orbits.

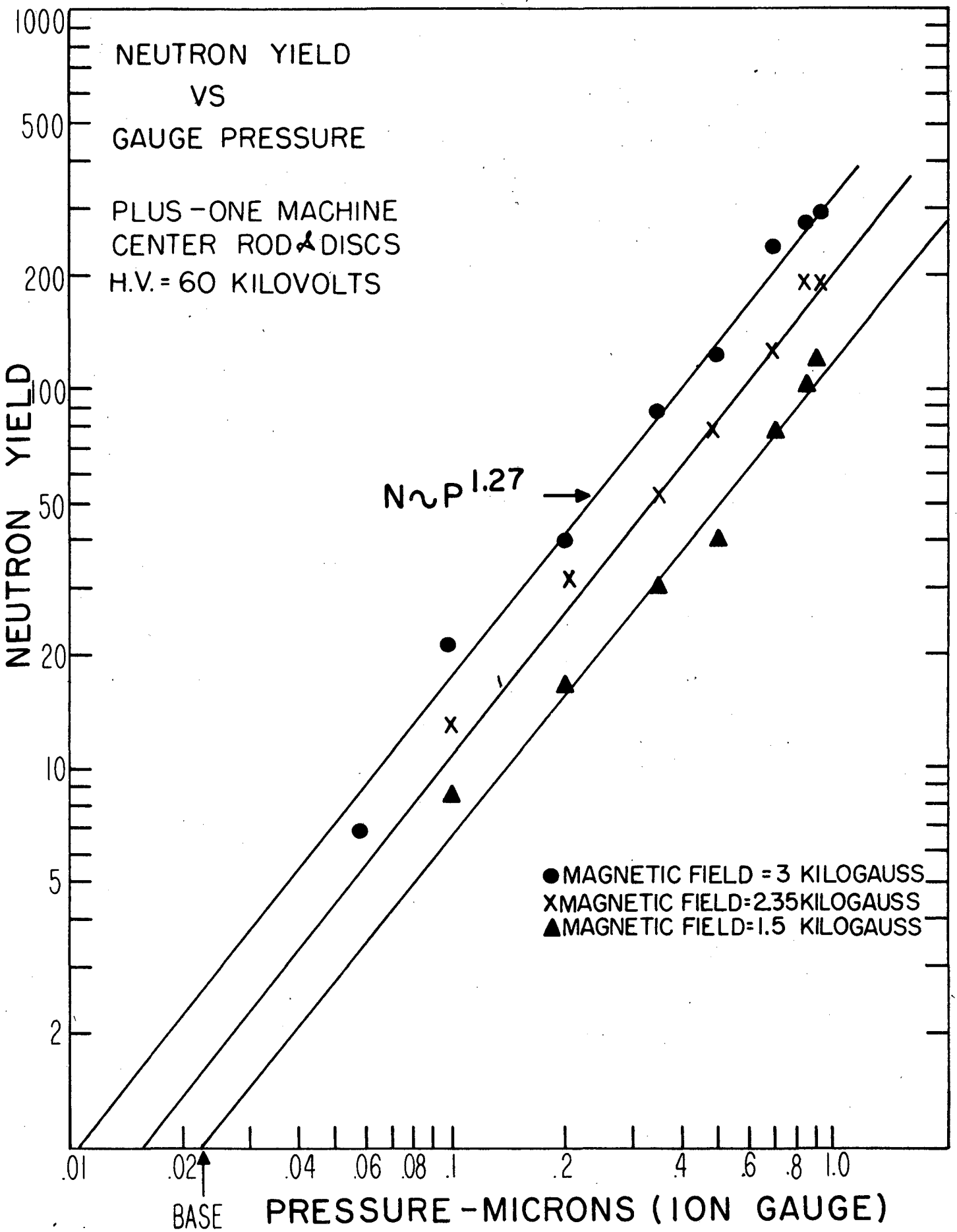
NEUTRON YIELD
VS
GAUGE PRESSURE
PLUS-ONE MACHINE
CENTER ROD & DISCS
H.V. = 60 KILOVOLTS
NEUTRON YIELD
1000
500
200
100
50
20
10
5
2
N∼P 1.27
●MAGNETIC FIELD = 3 KILOGAUSS
XMAGNETIC FIELD=2.35KILOGAUSS
▲MAGNETIC FIELD=1.5 KILOGAUSS
.01
.02
.04
.06
.08
.1
.2
.4
.6
.8
1.0
BASE PRESSURE
PRESSURE-MICRONS (ION GAUGE)

Fig. 9

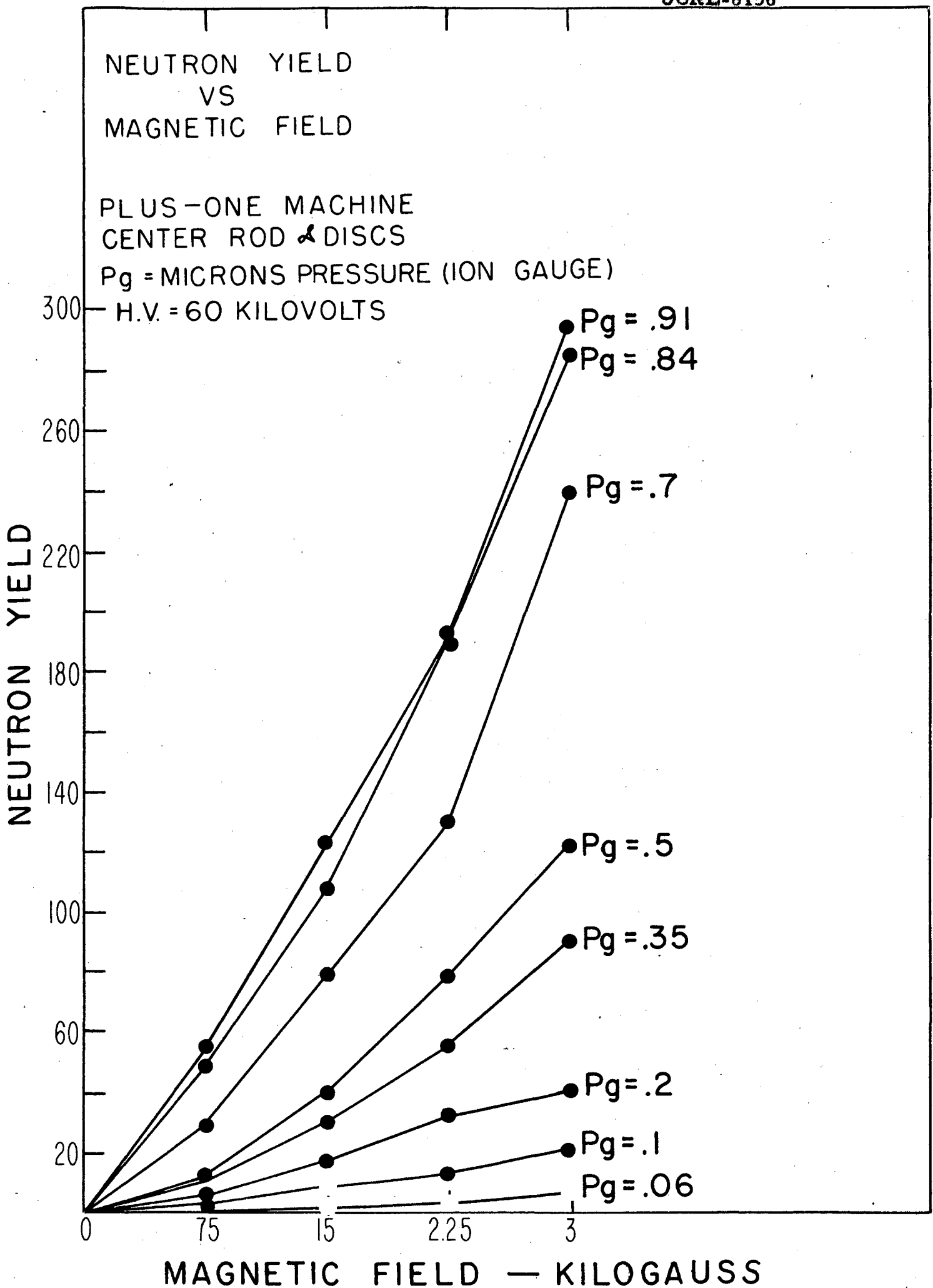

Fig. 10

50,604-1

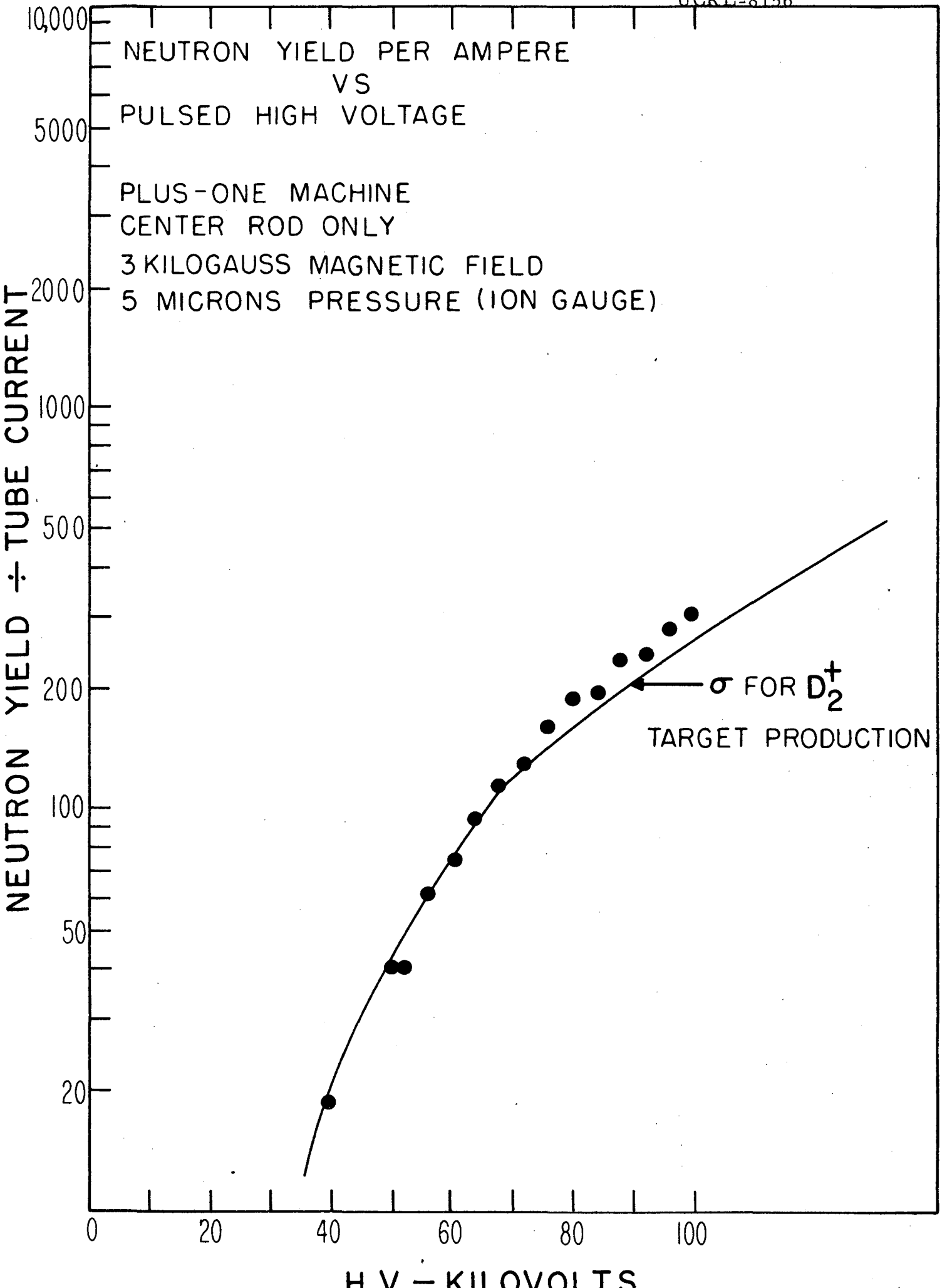

Fig. 11

5C. 601-1

PICK-UP ELECTRODES (FINS)
INSTALLED IN PLUS-ONE

SECRET

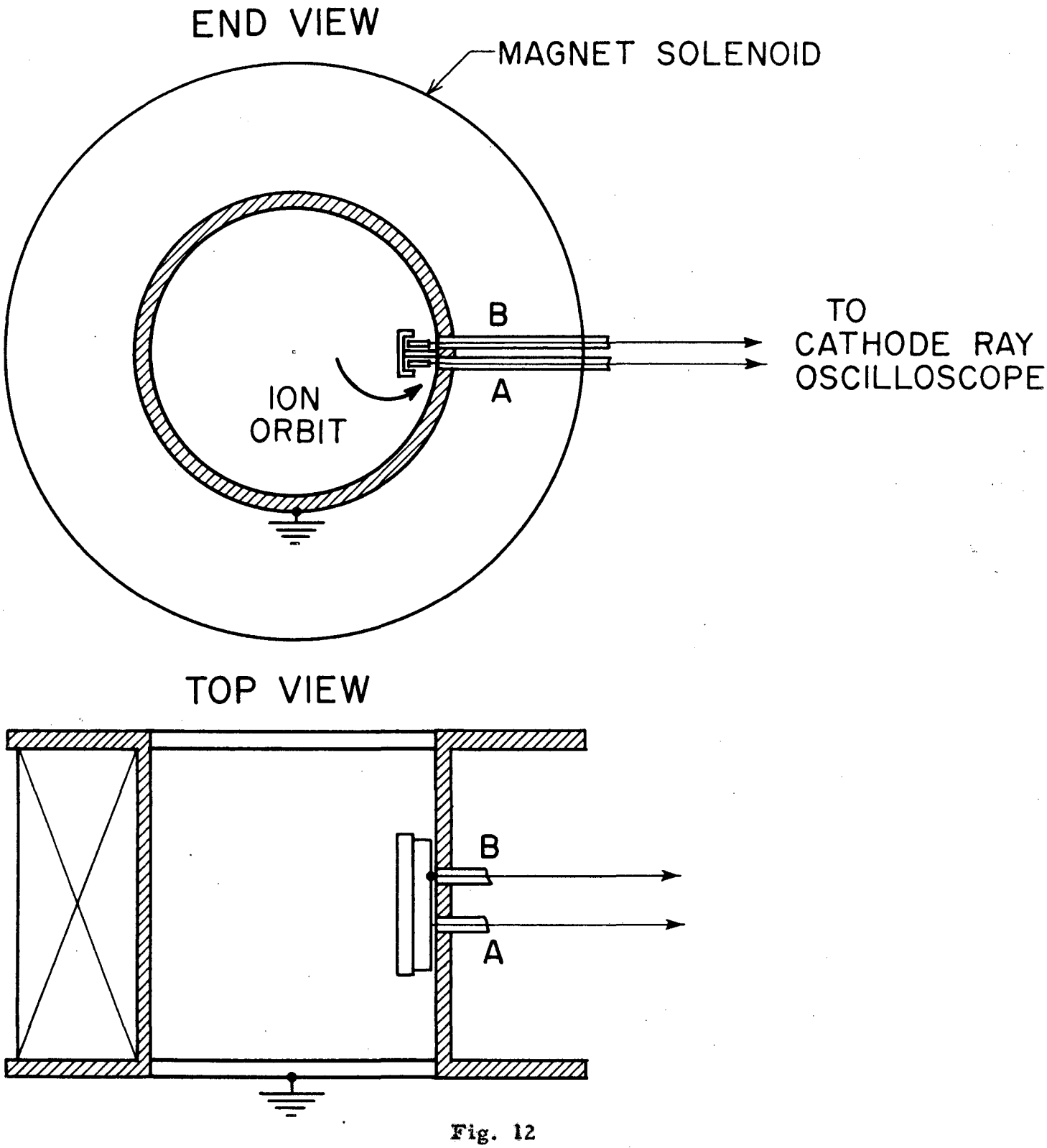

Fig. 12

The fins were also used as rf-pickup electrodes. For Plus-One with and without the central rod the principal frequency observed was about 15 to 20 megacycles. (The ion Larmor frequency is 2.5 Mc.)

For Plus-One without central rod, a burst of rf hash with frequency of about 1 Mc was observed to last for 5 msec after the high-voltage pulse. Sometimes the start of this burst would be delayed by 1 msec after the end of the voltage pulse. These delayed oscillations had an amplitude of one-tenth that of the 20-Mc oscillations observed during the high-voltage pulse. When the central rod was inserted in Plus-One, the delayed oscillations were not observed.

Plus-Three Experiments

For examining more carefully the effects occurring in the throat region without interference from the effects occurring near the end discs, a machine named Plus-Three was constructed as shown in Fig. 13. This machine consists of just the central rod and the solenoidal magnetic field. The magnet is pulsed with a rise time of about 0.1 sec, so that for a 100-μsec high-voltage pulse we have essentially a dc magnetic field. One end of the cylindrical vacuum system is terminated with a pyrex plate, so that visual and photographic observations can be made.

The neutron yield and tube current are plotted vs pressure in Fig. 14. The neutron yield goes as the pressure to the power 1.55. When Plus-Three is at its base pressure of 2×10^{-6} mm Hg, it still draws a current of 1.6 amperes. This is quite different from the behavior of Plus-One without central rod, which drew almost no current at low pressure. Presumably the central sheath did not form in Plus-One at low pressure.

The neutron yield vs voltage for Plus-Three is seen in Fig. 15 to go essentially as the cross section for D_2^+ ion bombardment of a thin target, as had been observed also for Plus-One. The neutron yield and tube current as a function of magnetic field are shown in Fig. 16. As the magnetic field is increased, there is an abrupt increase in the neutron yield, whereas the tube current is relatively constant. At the highest magnetic fields available the neutron yield seems to fall off slightly.

After the voltage pulse is applied to Plus-Three, the tube-current trace remains at zero for several microseconds, and then moves almost straight up to its final value. At lower pressures the delay in the current pulse is longer, as shown in Fig. 17. At very low pressures there is a variation of a few microseconds from pulse to pulse in the length of the delay. This delay in current pulse may correspond to the similar delay of about 1 μsec observed at much higher pressures in the Homopolar machine.[1]

When one looks through the pyrex end plate of Plus-Three the sheath surrounding the central anode rod can be observed. Outside the sheath there is a dark region, and then a bright "doughnut" with

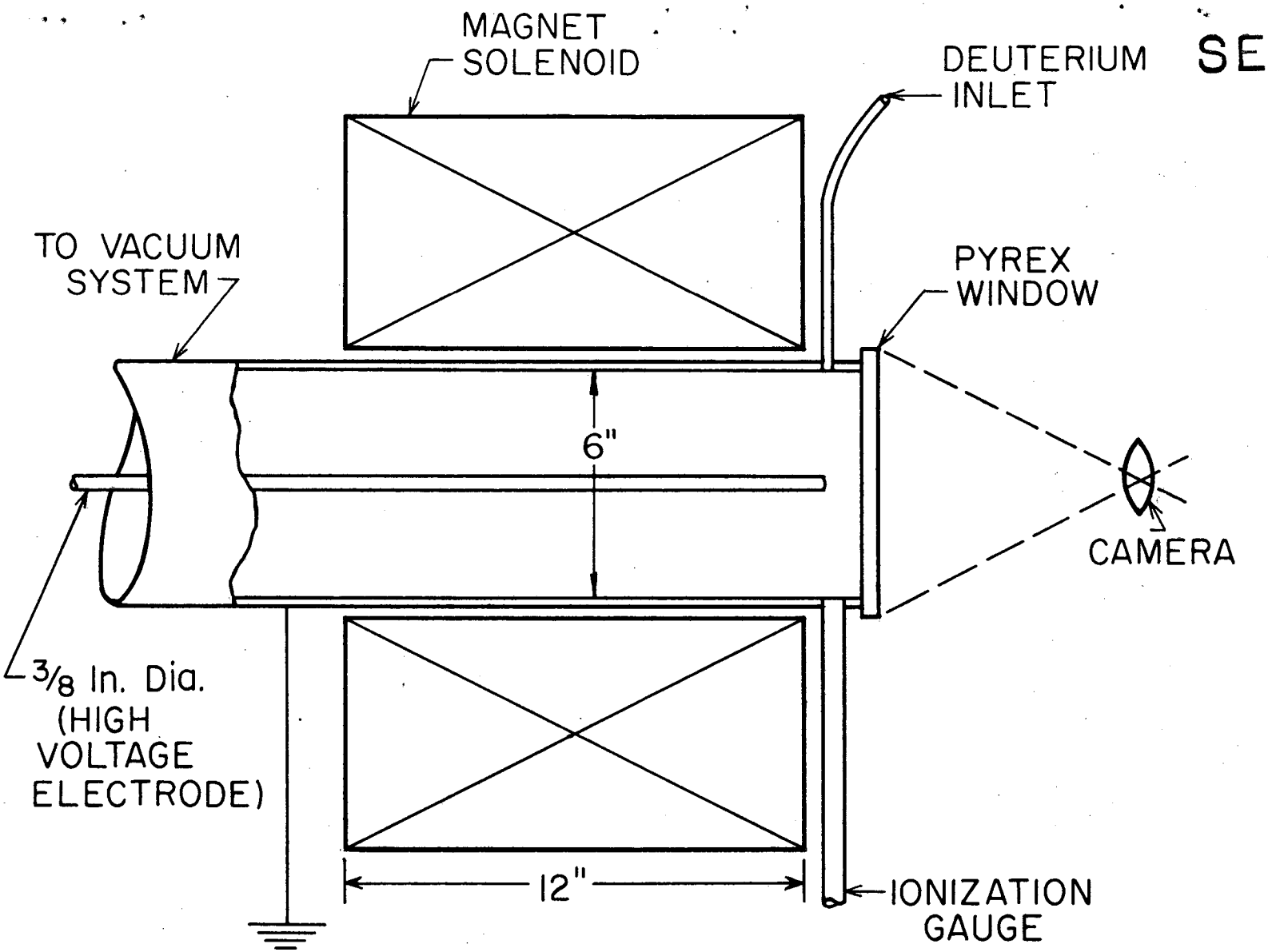

HIGH VOLTAGE PULSE

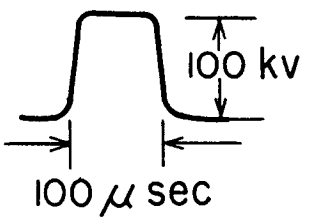

Fig. 13

UCRL-8156

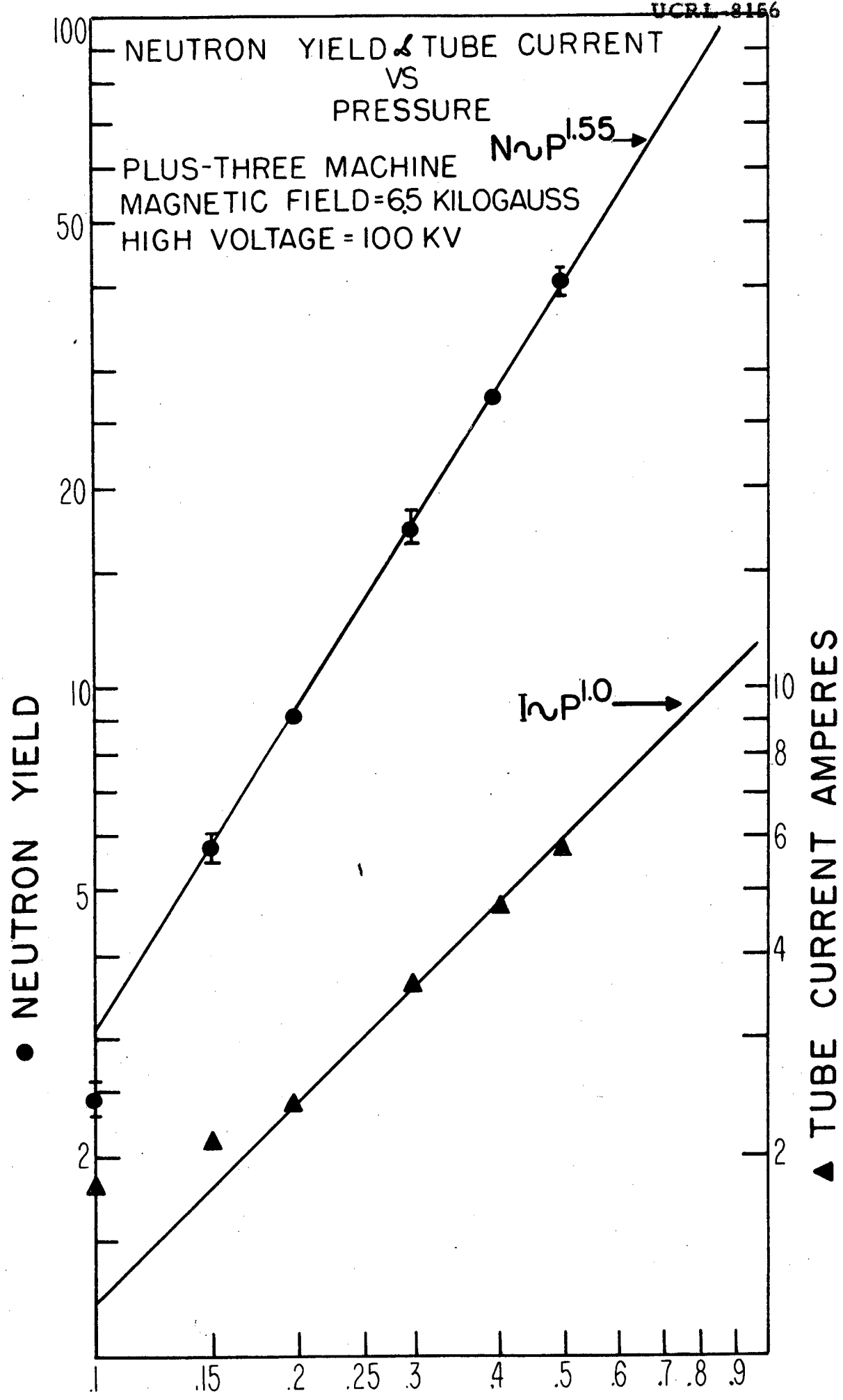
NEUTRON YIELD & TUBE CURRENT
VS
PRESSURE
PLUS-THREE MACHINE
MAGNETIC FIELD=6.5 KILOGAUSS
HIGH VOLTAGE = 100 KV
N∼P^1.55
I∼P^1.0
● NEUTRON YIELD
▲ TUBE CURRENT AMPERES
100
50
20
10
5
2
10
8
6
4
2
.1
.15
.2
.25
.3
.4
.5
.6
.7
.8
.9
PRESSURE MICRONS (ION GAUGE)

Fig. 14

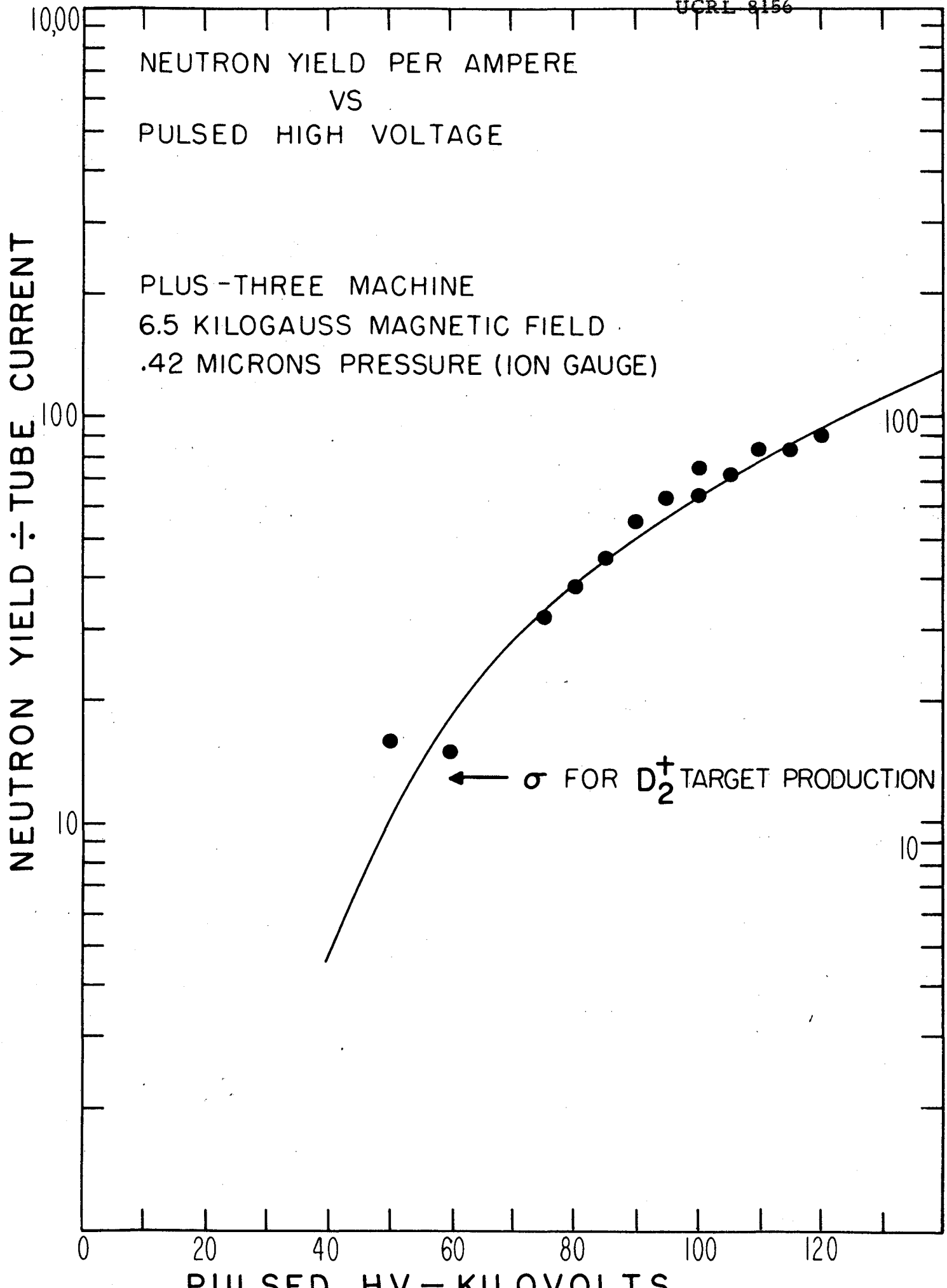

Fig. 15

5C.602-1

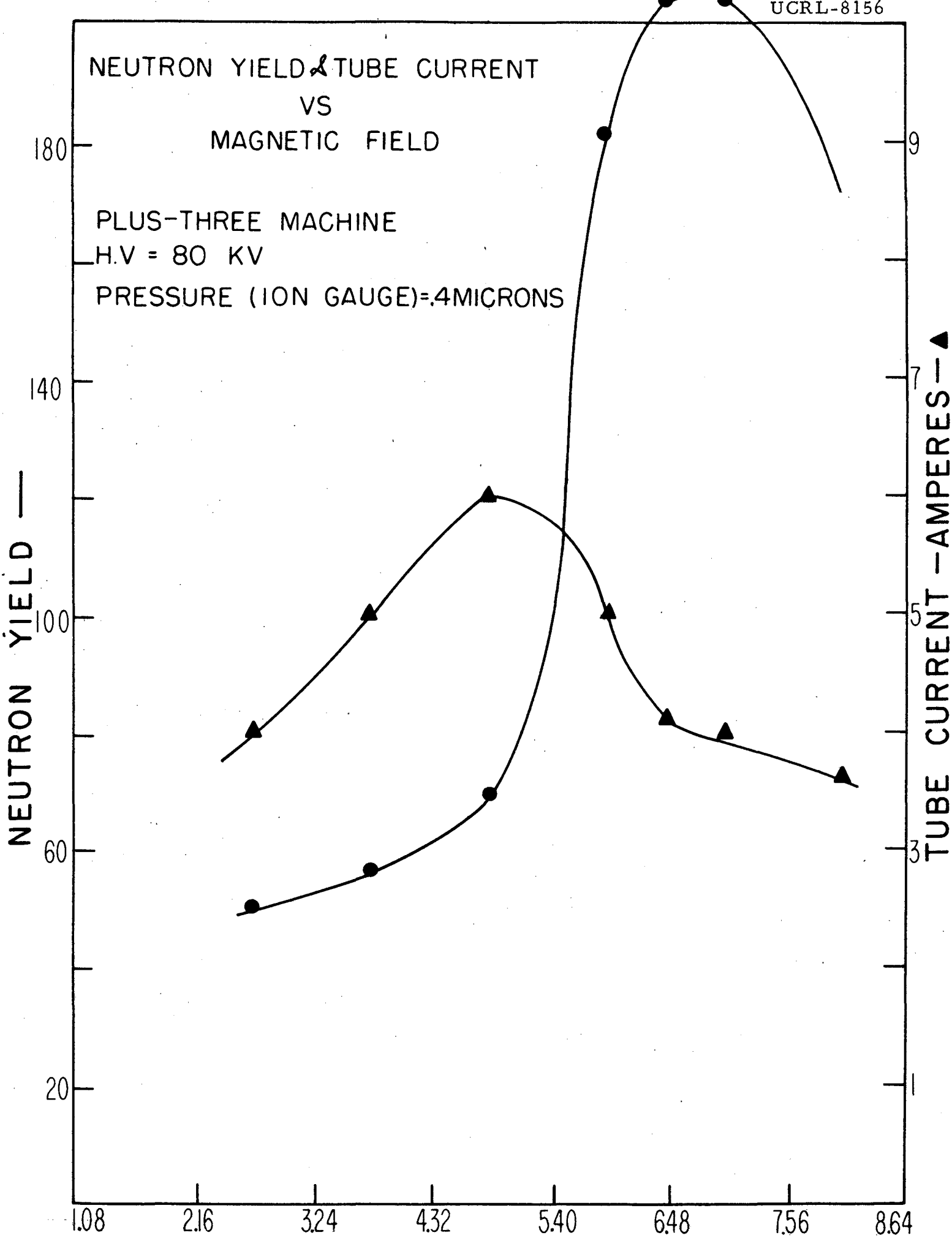
NEUTRON YIELD & TUBE CURRENT
VS
MAGNETIC FIELD
PLUS-THREE MACHINE
H.V = 80 KV
PRESSURE (ION GAUGE)=.4MICRONS
NEUTRON YIELD
180
140
100
60
20
TUBE CURRENT - AMPERES
9
7
5
3
1
1.08
2.16
3.24
4.32
5.40
6.48
7.56
8.64
MAGNETIC FIELD — KILOGAUSS

Fig. 16

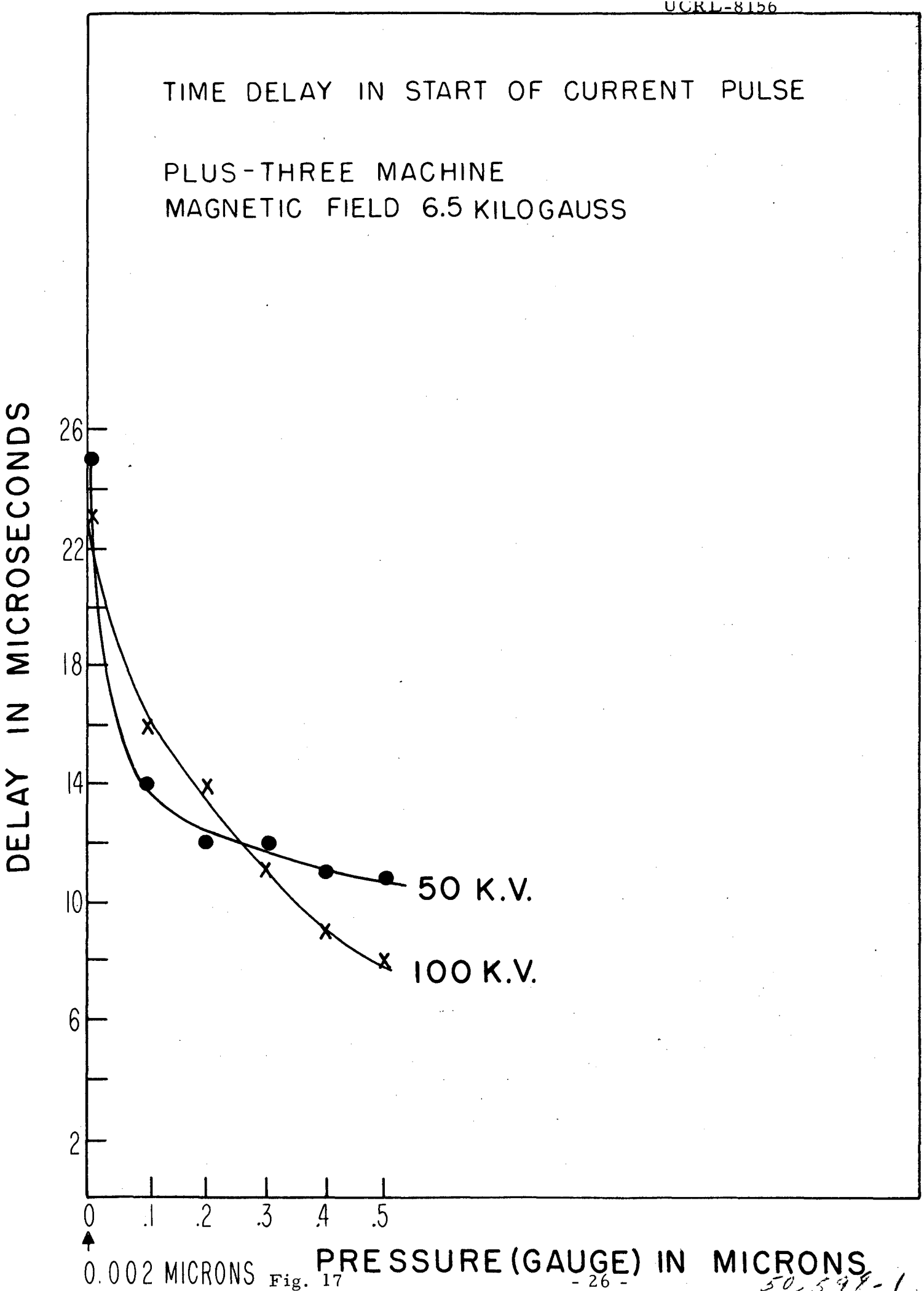

Fig. 17

50-598-1

an inner diameter of 4 cm at 6.5 kilogauss. Photographs of the discharge at four values of the magnetic field are shown in Fig. 18, and the thickness of the anode sheath as a function of magnetic field is shown in Fig. 19.

III. SHERWOOD APPLICATIONS: THEORETICAL

Since the devices described above operate at such low pressures that the mean free paths for most collision processes are long compared with the dimensions of the system and at such high voltages that the ion Larmor radii can be large compared with these dimensions, one must be cautious in applying familiar concepts such as the dielectric constant of a plasma or the effect of torques due to radial currents. We have instead developed the following rough picture of the way in which the discharge develops, which is consistent with the observed development of the sheath and accounts for the current that flows during the pulse.

Considering now Plus-Three or the throat region of Plus-One with central rod, when the voltage is first applied to the tube its radial distribution is that of a vacuum field (Curve I of Fig. 20). Any ions that exist are accelerated outward and reach the outer cylinder with very little deflection by the magnetic field. Any electrons, on the other hand, are restricted to excursions of a millimeter or less and thus remain essentially at the radial position at which they were born, but with sufficient average energy to produce further ionization. The new ions also reach the outer wall and the electrons still remain behind. As the negative space charge increases, the potential is depressed until at some point in radius it becomes equal to the magnetron cutoff potential for ions starting at thatradius (Curve II, Fig. 20). This probably occurs first at the outer radius (Curve III, Fig. 20), at a net electron density of the order of 10^9/cc. Ions created at smaller radii continue to leave, depressing the potential still further until the ion-cutoff condition is met at such a small radius that the newly produced electrons reach the inner conductor. This radius, r_s, is given approximately by a magnetron cutoff condition for particles accelerated inward:

$$r_s^2 \sim a^2 \left[1 + \sqrt{\frac{8eV}{m\omega_e^2 a^2}} \right],$$

where a = radius of inner cylinder,
V = applied voltage,
m = electron mass,
ω_e = electron cyclotron frequency in the applied magnetic field.

At this point an equilibrium is reached, with no further change in space-charge density ($\sim 10^{10}$ - 10^{11} electrons/cc), though a current continues to flow as the energetic electrons in the sheath continue to ionize the neutrals in that region. It is apparently this current of molecular ions, accelerated in the sheath, that produces the observed neutrons as

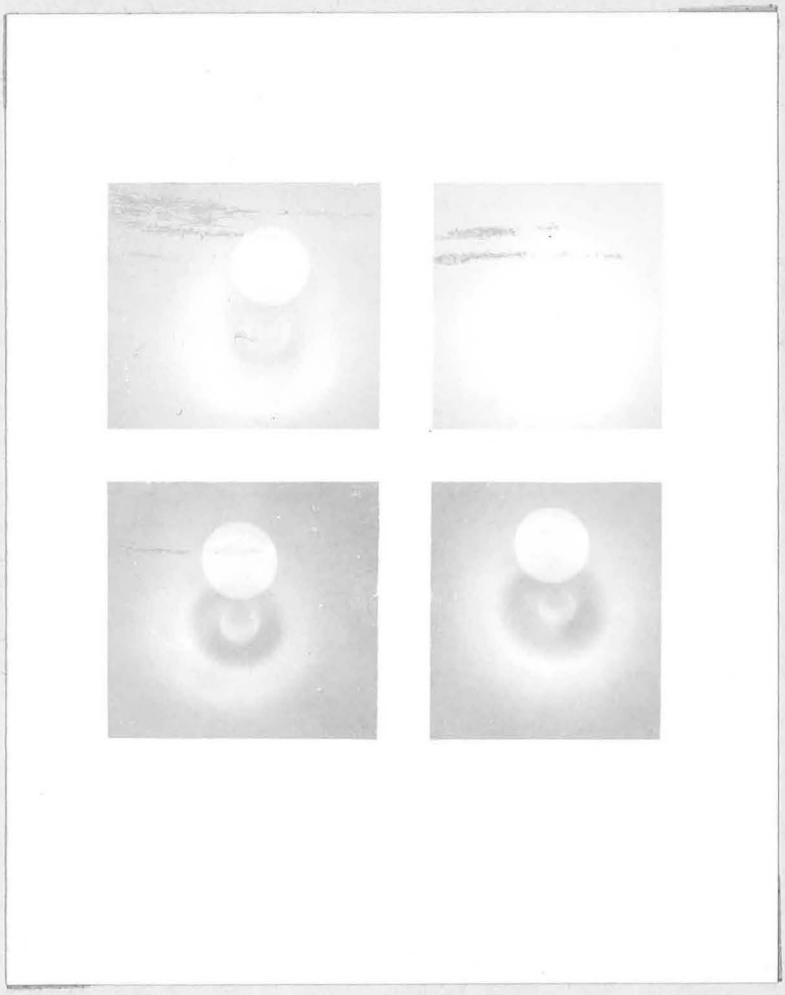

Fig. 18

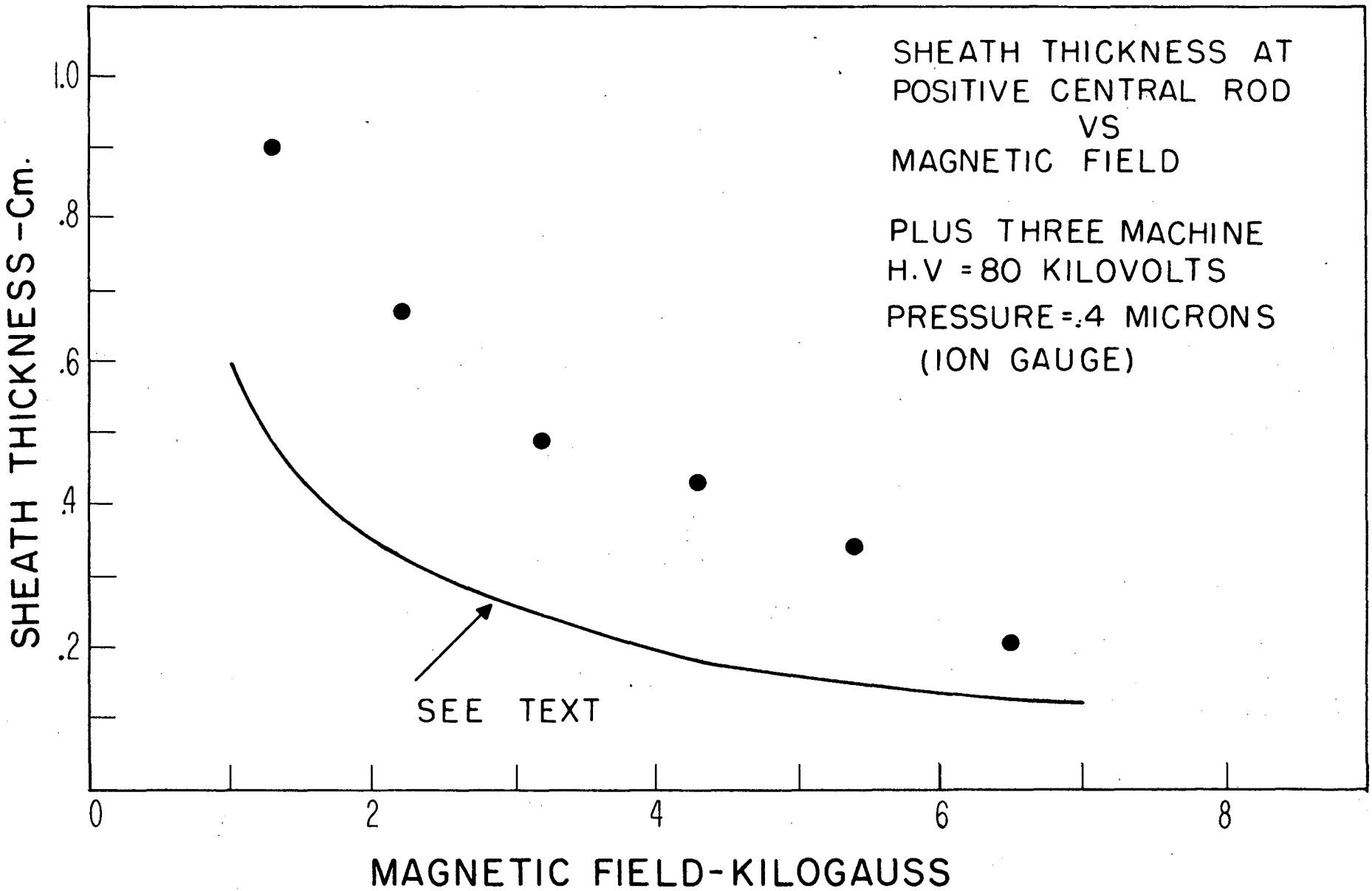

UCRL-8156

Fig. 19

50,605-1

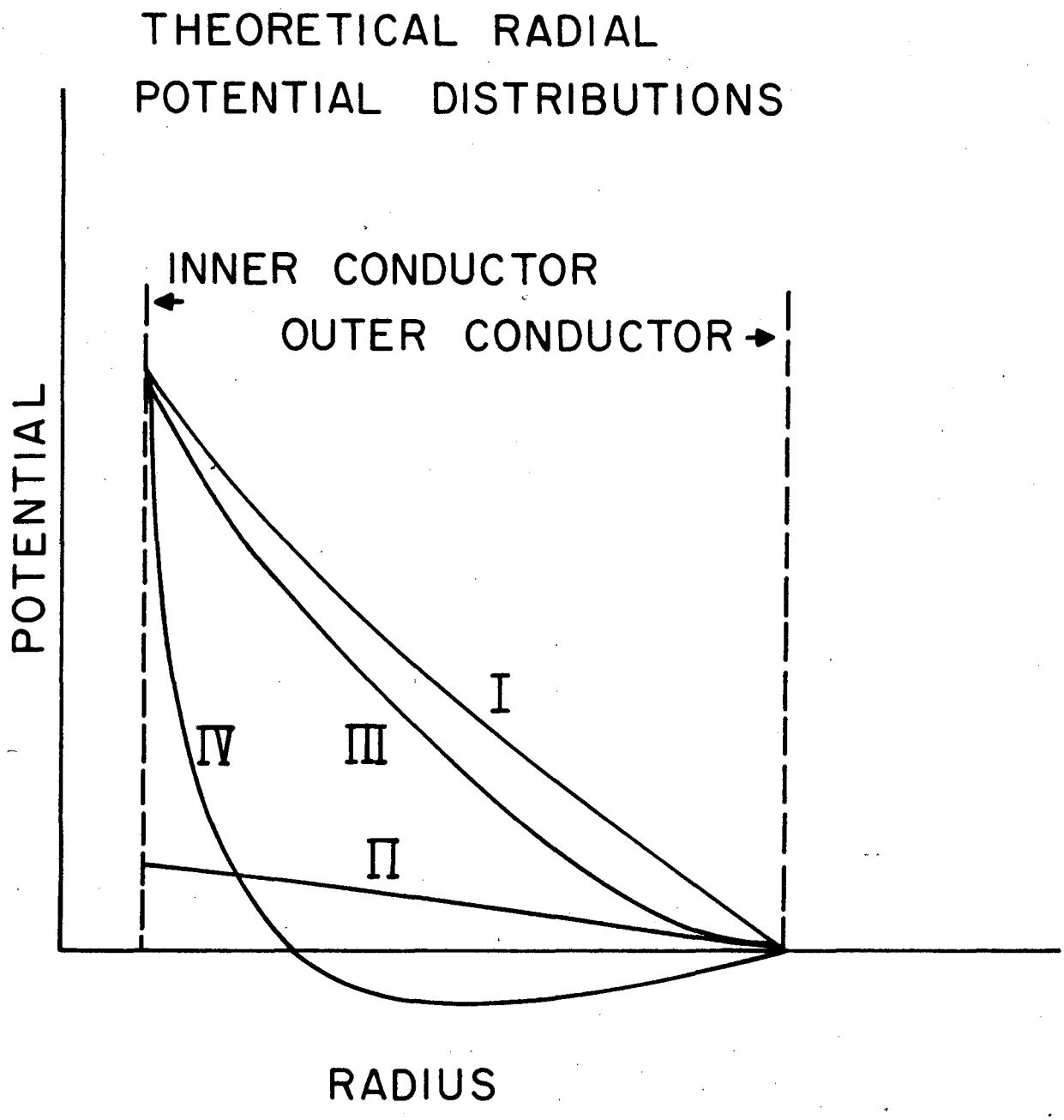
THEORETICAL RADIAL
POTENTIAL DISTRIBUTIONS
INNER CONDUCTOR
OUTER CONDUCTOR
POTENTIAL
I
II
III
IV
RADIUS

Fig. 20

it passes through the gas, or plasma, in the volume outside the sheath. The sheath is evidently self-stabilizing, in the sense that in the event of a fluctuation in space-charge density or applied voltage, ions or electrons leave the region until equilibrium is reestablished.

There are some quantitative checks that can be made of this picture. The delay in the start of current flow and its subsequent exponential rise are accounted for by considering the rate of ionization by electrons in cycloidal orbits. The total charge supplied by the external cricuit during the build-up of the sheath is due in part to the real ion current and in part to the change in capacity because of the trapped space charge. The more or less steady current during the remainder of the pulse is accounted for by the ionization rate of the sheath electrons.

Unfortunately it is not so easy to guess at what is going on in the region external to the sheath. As can be seen from Curve IV, Fig. 20, the above argument implies a tendency to form a potential well of considerable depth in the outer region, which would give rise to a sort of plasma oscillation in which the ions, being relatively free to move across the magnetic field, might acquire considerable kinetic energy. However, in order to claim a substantial plasma in the outer region, it is necessary to demonstrate a mechanism for axial containment, which we have been unable to do for the geometry of these devices, either experimentally or theoretically. Indeed it is more likely that charged particles will leave the throat region, where the magnetic field is strongest. [1]

A significant by-product of the considerations on sheath formation in that the only apparent function of a high applied voltage is to facilitate breakdown of the gas. Once the potential in the outer region has dropped below the magnetron cutoff value, the sheath serves only to cause a power drain and create unwanted neutrons.

IV. FUTURE PLANS

We would like to establish experimentally a situation wherein a considerable density of ions are trapped in magnetron-like orbits in the volume between the outer edge of the sheath and the outer diameter of the vacuum system. Since the orbits of particles starting from different places would be very complicated, collisions between rapidly moving ions would be expected.

A machine with mirror coils is being constructed in the hope of utilizing the mirror-enhancement properties pointed out by Furth. [1] We are also planning in a later machine to increase the outside diameter of the system from 6 inches to 16 inches. This would considerably increase the magnetron cutoff energy and should make any effects caused by ions in magnetron-like orbits easier to detect.

Oscillations with a frequency of about 20 Mc have been reported above. Careful observation of the effects on these oscillations of changes

in magnetic field, electric field, pressure, and ion mass may be useful for diagnostic purposes. We also plan to do more work with probes and pickup coils in an effort to better understand the distributions of potential and any induced magnetic fields.

Figure Captions

Fig. 1. Arrangement of electric and magnetic fields.

Fig. 2. Diagram of single-ended tube.

Fig. 3. Photograph of single-ended tube.

Fig. 4. Drawing of double-ended tube.

Fig. 5. Photograph of double-ended tube.

Fig. 6. Drawing of Plus-One.

Fig. 7. Graph of neutron yield and tube current vs pressure for Plus-One.

Fig. 8. Neutron yield vs voltage for Plus-One.

Fig. 9. Neutron yield vs pressure for Plus-One with central rod.

Fig. 10. Neutron yield vs magnetic field for Plus-One with central rod.

Fig. 11. Neutron yield vs voltage for Plus-One with rod only.

Fig. 12. Pick-up Electrodes installed in Plus-One.

Fig. 13. Drawing of Plus-Three.

Fig. 14. Neutron yield and tube current vs pressure for Plus-Three.

Fig. 15. Neutron yield vs voltage for Plus-Three.

Fig. 16. Neutron yield and tube current vs magnetic field for Plus-Three.

Fig. 17. Time delay in start of current pulse.

Fig. 18. Photographs of Plus-Three discharge.

Fig. 19. Sheath thickness at positive center rod vs magnetic field.

Fig. 20. Theoretical potential vs radius. Upper left, 6.5 kilogauss; upper right, 5.4 kilogauss; lower left 4.3 kilogauss; lower right, 3.2 kilogauss.

Reference

1. Anderson, Baker, Bratenahl, Furth, Ise, Kunkel, and Stone, The Homopolar Device, UCRL-8062, Jan. 1958.